Trop J Nat Prod Res, July 2025; 9(7): 3150 - 3159 **ISSN 2616-0684 (Print)**
ISSN 2616-0692 (Electronic)

Tropical Journal of Natural Product Research

Available online at https://www.tjnpr.org

Original Research Article

Green Synthesis of Silver Nanoparticles with Silkworm Excretions and their Potential Antibiofilm Activity on Oral Bacteria

Qutaiba A Ismael[1], Mohammed S Ali[1], Raghda H Aljorani[2], Ali Al-Shammari[3], Mohammed H Al-Bayati[1]

[1]*Department of Pharmaceutics, College of Pharmacy, Al-Farahidi University, Baghdad, Iraq*
[2]*Department of Clinical Chemistry, Faculty of Pharmacy, Al-Rafidain University College, Baghdad, Iraq.*
[3]*Department of Pharmaceutics, Faculty of Pharmacy, Al-Nahrain University College, Baghdad, Iraq.*

ARTICLE INFO

Article history:
Received 05 April 2025
Revised 06 June 2025
Accepted 14 June 2025
Published online 01 August 2025

ABSTRACT

Dental caries is a chronic infectious disease that causes tooth loss and root breakdown in children and young adults, with a prevalence ranging from 60-80% in children and almost 100% in adults. Green synthesis of metallic nanoparticles is a highly economical and practical way to reduce antimicrobial resistance. Green synthesis of silver nanoparticles (AgNPs) was performed using silkworm pellets and validated by characterization studies (UV-visible spectroscopy, XRD, FTIR, and SEM). Antibacterial activity was evaluated against three oral bacterial strains (*S. mutans*, *S. oralis*, and *S. gingivalis*) by MIC, time-kill, and antibiofilm assays. qRT-PCR was performed to evaluate the expression of biofilm-formation genes (gftB, gftC, gftD, srtA, and comD). Scanning electron microscopy (SEM) showed that the synthesized AgNPs were between 40 and 55 nm (in). The synthesized AgNPs were found to reduce biofilms and exopolysaccharides in accordance with the MIC and agar well diffusion. Antibacterial activity was found to be highly significant with NPs, as evidenced by the downregulation of the qRT-PCR genes. The green-synthesized AgNPs from silkworm excreta exhibited antibacterial activity against oral bacteria, with a high percentage of biofilm inhibition and downregulation of biofilm-forming genes.

Keywords: Antibacterial activity, Extracellular polysaccharide, Oral bacteria, Reverse transcription polymerase Chain reaction, Silkworm excreta.

Introduction

Dental caries is a persistent, localized illness that causes changes in the tooth structure as a result of chemical loss from metabolic activity and the development of dental biofilms on the tooth surface1. Initially, this transformation was reversible. Saliva intake, sugar intake from food, and fluoride exposure are among the many variables that affect dental caries outcomes.[2] These variables affect the dynamic equilibrium between demineralization and remineralization processes. Dental caries are now categorized as diseases such as cancer or diabetes with multiple etiologies and no single mechanism of cause. Soon after birth, the infant's mouth begins to colonize with oral microbes. Due to exposure to microbial sources from outside the world, the number of oral bacteria has steadily increased. *Streptococcus salivarius*, *Streptococcus mitis*, and *Streptococcus oralis* were the earliest and most prevalent oral bacteria to colonize the oral cavities of newborn infants. Following the eruption of primary teeth, the number and variety of oral microbiota have increased.[3]

*Corresponding author. Email: raghda.khalil@ruc.edu.iq
Tel: (+964)7906302268

Citation: Ismael QA, Ali MS, Aljorani RH, Al-Shammari A, Al-Bayati MH. Green Synthesis of Silver Nanoparticles with Silkworm Excretions and their Potential Antibiofilm Activity on Oral BacteriaTrop J Nat Prod Res. 2025; 9(7): 3150 – 3159 https://doi.org/10.26538/tjnpr/v9i7.39

Official Journal of Natural Product Research Group, Faculty of Pharmacy, University of Benin, Benin City, Nigeria

Typically, nanoparticles have sizes between 1 and 100 nm. Atomic clusters, nanorods, spots, grains, fibers, films, and nanopores with large surface areas are possible manifestations. Compared with traditional materials, these materials exhibit better physicochemical characteristics. Nanoparticles have antiviral, antifungal, and antibacterial properties. Nanoparticles may also improve the mechanical characteristics, prevent crack spread, and boost the fracture toughness of dental materials. Consequently, the use of nanoparticles in dentistry has increased. [4] Nanoparticles are effective in periodontology, implantology, endodontics, prosthetic dentistry, implantology, preventative dentistry, restorative dentistry, and oral cancer. According to recent research, metallic nanoparticles can prevent dental caries by lowering biofilm development and demineralizing carious lesions. Metallic nanoparticles promote the remineralization of demineralized (carious) tooth tissues, which promotes biomineralization. Owing to their ion balance in oral fluids, metallic nanoparticles can overcome the difficulties associated with various oral disorders. [5] According to Hoque et al., glucosyltransferases (GTFs) are essential for the synthesis of *S. mutans'* soluble and insoluble extracellular polysaccharides (EPSs).[6] The EPSs help S. mutans adhere to teeth and promote the growth of biofilms, making them resistant to antibiotics. [7] Therefore, inhibition of EPS production can hinder the growth of biofilms and reduce the frequency of dental caries. Dental caries is a serious public health concern worldwide. Currently, the mechanical removal of oral biofilms remains the best method for preventing dental caries and periodontal illnesses. The use of antibiotics has provided medical professionals with new ways to combat dental caries. [8] Due to the medication resistance of some bacteria, the use of antibiotics alone cannot completely prevent demineralization and may even result in infection. A significant factor in the failure of antimicrobial therapy and the development of antibiotic resistance is the creation of microbial biofilms such as dental plaque. [9] However, the molecular processes that drive biofilm cell survival remain poorly understood. There are three possible causes for this problem: the first is biofilm-specific defense against oxidative stress; the second is the expression of efflux pumps that release antibiotics

specifically in biofilms; and the third is the defense offered by matrix polysaccharides that can reduce antibiotic diffusion and may have a significant impact on antibiotic resistance.[10] The rational use of antibiotics has been advocated for, [11] health systems and regulatory capacity have been strengthened,[12] and new antibiotics and other antibacterial drugs have been explored,[13] among other proactive strategies for bacterial resistance. Because it is exceedingly challenging for AgNPs to cause bacterial resistance, AgNPs are currently receiving a lot of attention as antibacterial agents. For clinical translational use, it is critical to manufacture nanomaterials in a secure, sustainable, and cost-effective manner. [14] Green synthesis is one of several AgNP preparation techniques that have attracted attention. In this study, the antibacterial activity of green-synthesized AgNPs from silkworm excreta/pellets against three oral bacterial species, *S. mutans, S. oralis*, and *S. gingivalis* was investigated. The antibacterial activity was evaluated using MIC, time-kill assays, antibiofilm studies, and RT-PCR of biofilm-forming gene members.

Materials and Methods

Collection of silkworm excreta
The Silkworm pellets were collected from Al-Mustansiriyah University, College of Pharmacy.

Bacterial strains
S.mutans (MTCC 729), *S. oralis* and *S. ginigivalis* were purchased from MTCC, India. Antibiotics and media were purchased from HiMedia, Ltd. (India). Bacteria were revived and subcultured in Mitis salivarius base at 37°C for 12-18 hours and maintained as a pure stock.

Extraction of the sample
Silkworm excreta/pellets were pulverized into a fine powder and filtered through a sieve. Approximately 10 g of the powder was added to 100 ml of distilled water and magnetically stirred for 24 h at 200 rpm. Following incubation, the mixture was filtered through Whatman No. 1 filter paper and centrifuged at the maximum speed for 10 min. The collected supernatant was used for the green synthesis of AgNPs.

Green synthesis of AgNPs
An aqueous silver nitrate solution (0.1 mM) was prepared for the synthesis of AgNPs. 14 An equal volume of the extract and silver nitrate solution was added to a conical flask and stirred at 200 rpm overnight at 45°C until the color changed. The reduction of silver ions to AgNPs was confirmed by the color change. The solution was centrifuged at the maximum speed to pellet the SEAgNPs. The pellet was dried in a hot-air oven and stored for further use. The synthesized SE-AgNPs were characterized by UV-visible spectroscopy, XRD, FT-IR, and SEM.

Nanoparticle characterization
AgNP production has frequently been studied using UV-visible spectroscopy. The SEAgNPs were characterized using a UV spectrophotometer (Shimadzu, 1800). The agents present in the extracts around the synthesized SEAgNPs were subsequently classified using a Fourier transform infrared (FT-IR) spectrometer at 500–4000 cm^{-1} (Shimadzu, Koyoto, Japan) after the SEAgNPs were freeze-dried. DLS model SZ-100 was used to measure the polydispersity index (PDI) and size distribution of the synthesized SEAgNPs under scattered light at angles of 90°or 173 °(default) at a speed of 3° min-1 and a step size of 0.02° in the 2θ range of 10° to 70°.

Zeta potential measurements were done at a temperature of about 25ºC to verify the dispersion and general stability of the synthesized AgNPs. The size and distribution of the synthesized nanoparticles were investigated using nanoparticle tracking and analysis (NTA) LM-20 (NanoSight Ltd., UK). Because NTA aids in particle separation based on size and intensity, it also determines the Brownian motion of particles. A Horiba SZ-100 analyzer (Kyoto, Japan) was used to screen the hydrodynamic size (Z-average), polydispersity index (PDI), and surface charge (zeta potential) of green-synthesized SEAgNPs. Particle size analysis was carried out at a medium count rate of 210kCPS and scattering angle of 90° at approximately 25°C. Scanning electron microscopy (SEM) was used for the morphological analysis. The morphology of the green synthetic SEAgNPs was investigated to identify whether aggregates had developed.

Antibacterial activity
Well diffusion method
The well diffusion method was used to test the antibacterial activities of the synthesized SEAgNPs according to the National Committee for Clinical Laboratory Standards (NCCLS). [15] Three selected oral bacterial strains (SM, SO, and SG) were grown in Mitis salivarus broth for18 hr. The bacterial isolates were generated by keeping the colony-forming units (CFU) at 1.5 x 108/ml. Bacterial suspensions were applied to nutrient agar (NA) plates after preparation. A cork borer was used to drill wells (9 mm in diameter) into NA plates. Each well received 50µl of SEAgNPs at different concentrations (20µg/ml and 40µg/ml). The plates were incubated at 37°C for 24 h. The zone of inhibition was measured in millimeters (mm). The experiments were performed in triplicates. The means and standard deviations were used to express the data.

Broth dilution assay
The two-fold dilution method was used to determine the minimum inhibitory concentration (MIC) of the SEAgNPs as described previously. [16] All three bacterial isolates were diluted to 2 × 106 CFU/ml in MSB. Broth dilution assay was performed using a 96-well titer plate. Approximately 10 µl of the diluted culture (106 CFU/ml) was added to each well of the plates containing 180 µl of MSB. Approximately 10 µl of the inoculum was added to each well. Sterile distilled water was used as the negative control. Following inoculation, the plates were incubated overnight at 37°C and the absorbance was recorded at 600 nm using a microplate reader (Genetix, USA). Vancomycin (10 mg/ml) was used as a positive control. MIC was established as the lowest SEAgNP concentration that prevented bacterial growth. The minimum bactericidal concentrations (MBCs) were determined by plating bacterial suspensions from the MIC assay wells at SEAgNP concentrations equivalent to or higher than the MIC values on solid agar. MBC was determined by taking the lowest peptide concentration at which no bacterial growth appeared on the plates, following incubation. [15] All sets were conducted in triplicate.

Time-Kill Assay using SEAgNPs
The time-kill assay was performed as described by Abraham.[17] The three bacterial strains in the logarithmic phase were diluted in MSB to obtain a concentration of 1.5 × 106 CFU/ml. The SEAgNPs were diluted two-fold in phosphate-buffered saline (PBS). To 5 ml of MSB, 200 µl of SEAgNPs at varying concentrations (0.5, 1, and 2 MIC) were added, and 100 µl of each bacterial suspension was added to each well and mixed thoroughly. 18 The contents were incubated overnight at 37 °C for 0, 30, 60, 90, 120, or 180 minutes. Sterile distilled water was used as the negative control. Following incubation, 20 µl of each tube was plated onto MSA plates (1:50 dilution). The plates were incubated overnight at 37°C.

Antibiofilm activity of SEAgNPs
The effect of SEAgNPs on biofilm formation by the SM, SO, and SG strains was evaluated. [15] All the strains were grown to logarithmic phase in MSB at 37°C and diluted in MSB (supplemented with 3% sucrose). Approximately 1 × 106 CFU/mL of SM, SO, or SG were seeded into their respective wells containing 180 µl of MSB (HiMedia). Ten microliters of SEAgNPs at 2 × MIC was added to each well. Sterile distilled water was used as the negative control. A positive control (vancomycin, 10 mg/mL) was added to each well at similar concentrations. The plates were then incubated overnight at 37°C.The biofilm was analyzed using crystal violet and methyl thiazol tetrazolium (MTT) assays .[18] Following incubation, the wells were washed three times with PBS (pH 7.2) to remove bacteria that were not attached to the well. The biofilms were stained with CV (0.5%) for15 min and the

CV-stained biofilms were washed with ethanol:acetone (80:20). After washing, absorbance was measured at OD560 using a microtiter plate reader (Genetix, Germany). For the MTT assay, biofilms formed were washed and air-dried for 10 min. To the wells, 5µl of MTT (5 mg/ml) dissolved in 100µl of DMSO was added and incubated for 3 h at 37°C. The supernatant was collected and the absorbance of the purple color was recorded at 560 nm using a microtiter plate reader (Genetix, Germany). The lowest concentration at which biofilm formation was inhibited by at least 50% is known as the minimum biofilm inhibition concentration (MBIC50).

Biofilm Observation by Light Microscopy

S. mutans biofilms treated with GHc or GHd were observed by light microscopy, as previously described, with minor modifications. [19] In brief, SM, SO, and SG were cultured to the exponential phase (2 × 106 CFU/ml) with MSB (with 3% sucrose). Approximately 100 µl of each strain was seeded in wells containing circular coverslips. The cells were treated at 2MIC concentration and incubated at 37°C for 24 h. Following incubation, the biofilm inhibition protocol was performed as described in the previous section. After staining and destaining, coverslips were gently removed from the wells and air-dried. The biofilms formed were observed under a light microscope (Lawrence and Mayo, India).

Extraction of Extracellular Polysaccharides

The Bacterial EPSs from SM, SO, and SG isolates were isolated as previously described, with slight modifications. 20 Since peptides at concentrations near the MIC might decrease bacterial viability and interfere with the results, sub-MIC concentrations were used to ensure that bacterial growth was not affected. Approximately 1 ml of isolates (2 × 106 CFU/ml in MSB containing 1% sucrose) were treated with 0.5 MIC of SEAgNPs and incubated overnight at 37°C. Following incubation, the culture was centrifuged at 9,000 rpm for 10 min at 4°C. The resulting pellet was washed three times with water and the water-soluble glucan-containing supernatant was collected. After washing all the precipitates with 10 ml of 0.1 M NaOH, they were centrifuged at 10,000 rpm for 20 min. To precipitate out the water-insoluble glucans, the supernatants were then combined with 30 ml of cold 95% ethanol and left overnight at 4°C. The quantity of EPSs was measured using the phenol-sulfuric acid technique. EPSs were combined with equal volumes of aqueous phenol (5%) and sulfuric acid, and the mixture was then heated to 25°C. Absorbance was recorded at 490 nm using a microplate reader (Genetix, Germany).

RNA extraction

Gene expression was performed using RT-qPCR.15 In brief, approximately 200 µl of the isolate (2 × 107 CFU/ml) was added to 50µl of SEAgNPs (2 MIC) and incubated at 37°C overnight. Manual instructions for RNA extraction are also provided. The cultures were centrifuged at 5000 xg for approximately 5 min at 4°C, and the resulting supernatant was discarded. Approximately 500 µl of Buffer RLT was added to the pellet and vortexed. The contents were then centrifuged at full speed for approximately 10 seconds and collected in a new tube. An equal volume of 70% ethanol was added to the spin column after mixing thoroughly. After centrifuging the contents for 15 s (9000 g), the eluate was discarded. Approximately 700 µl of Buffer RW1 was added to the column and centrifuged for 15 s (9000 × g). The spin column was washed with 500 µl of Buffer RPE and centrifuged for 15 s (9000 × g). RNase-free water (30–50 µl) was added to the column and RNA was extracted after centrifugation for 1 min at 9000 rpm. RNA quality was assessed using a UV spectrophotometer (260/280 ratio) and was used to synthesize complementary DNA (cDNA).

cDNA synthesis

The SuperScript TMII Reverse Transcriptase, 200 U/µl (HiMedia) RT PCR kit was used to generate cDNA. Briefly, the initial reaction was initiated using approximately 2 µg of RNA obtained in the preceding phase. The volume retrieved was 1.56 µg/l. Therefore, 1.34 µl total RNA, 1 µl of RT enzyme, and random primers. The mixture was combined before incubation at 25°C for 10 min. The generated cDNA was stored for further use in gene expression after 45 min of incubation at 70°C.

Real-time PCR

Primers were used as previously mentioned and purchased from Sigma Ltd.. The iQTM SYBR Green Supermix (HiMedia) was used to conduct real-time PCR experiments in accordance with Durso (2014). primers (600nM) and 1µl of RT products were used in the PCR experiment, and a total volume of 12.5µl was used for the reaction. To verify the positive amplification, each reaction was conducted in triplicate and concurrently with the corresponding negative control.

Gene Expression

The samples (treated and control) were quantified in real time using a Corbett Research Cycler (Bio-Rad). The amplification program used primers gftB, gftC, gftD, sortase A, and comD at a concentration of approximately 600nM. The program was performed for approximately 40 cycles at 92°C for 50s, 64°C for 45s, and 72°C for 50s using 1.34µl of the RNA products. To compare mRNA expression, the housekeeping gene, recA, was amplified along with the relevant genes of interest. Using the Ct technique (ΔΔCt method), The relative amounts of mRNA in the test samples (including the control) were compared using the ΔΔCt method. The Ct values of the genes of interest were acquired and normalized to those of the housekeeping genes. [21]

Statistical Analysis

Each experiment was performed in triplicates. Data were analyzed using two-way analysis of variance (ANOVA) when appropriate, and differences between samples were verified using Tukey's test ($P \leq 0.05$) and were regarded as statistically significant. Analyses were conducted using SPSS software (version 20) throughout the investigation.

Results and Discussion

In the present investigation, SEAgNPs were formed from silver nitrate through the reducing action of the aqueous extract, as confirmed by the UV-visible spectra shown in Figure 1. The production of AgNPs was indicated by an absorption peak at approximately 436.54 nm. The large absorbance peak in the results, centered at 436 nm, could be attributed to the surface plasmon resonance band of the AgNPs. According to a different study, silkworm cocoon extract was gradually oxidized by silver ions when the concentration of $AgNO_3$ was raised [He H, 2017]. The structures of the SEAgNP samples were characterized using FTIR spectroscopy. The figure shows the original spectra of $AgNO_3$ and SEAgNPs. From the FTIR data, absorption bands for mM $AgNO_3$ solution at 832, 1210, 1420, 1540, and 3423 cm^{-1} was founded (Figure 2). Similar bands were reported, but with slight deviations from previously reported data.[22] The SEAgNPs represented the peak of Amide I at 1540 and 1420 cm^{-1}. Amine N–H stretching vibrations were observed at 3423 and 3410 for AgNPs and SEAgNPs, respectively. Two small bands were observed for the SEAgNPs at 2950 and 2780 cm^{-1}.

Additionally, the X-ray diffractogram clearly shows that the SE extract reduced Ag^+ ions to Ag^0 to generate AgNPs. The (111), (210), and (200) planes of silver are thought to be responsible for the characteristic diffraction peaks at scattering angles (2 θ) of approximately 38.8°, 43.2°, and 66.2°, respectively (Figure 3). The resulting particles were face-centered cubic structures of metallic AgNPs, according to previous studies. [23] This discovery makes it evident that AgNPs produced by the redox-active properties of tyrosine residues during the reduction of Ag^+ to Ag^0 are crystalline in nature.

ISSN 2616-0684 (Print)
ISSN 2616-0692 (Electronic)

Table 1: The list of primers used in the study

Gene		Sequence	Length	Tm	GC%	Product	Reference
gtf B	FW	TGCCGCAGTCCCTTCTTATTC	21	58.76	50	240	[31]
	RV	GCCATGTATTGCCCGTCATCT	21	58.73	50		
gtfC	FW	GTGCGCTACACCAATGACAGAG	22	58.99	50	210	[31]
	RV	GCCTACTGGAACCCAAACACCTA	23	59.05	55		
gtfD	FW	TACCTTGGGCACCACAACACT	21	59.05	60	150	[31]
	RV	TGCCGCCTTATCATCCTCACT	21	58.99	50		
Sortase A	FW	CACAACAAGGCTGCCCATTC	20	60.04	55	470	[15]
	RV	ATTGTTCTAGCAGTCGCCCC	20	60.11	55		
comD	FW	GCGATTGGAGCCTTTAGTGG	20	58.98	55	217	[15]
	RV	GCCTGAGATGGAGTTGCTTG	20	58.91	55		
**recA*	FW	ATCTCCGTCAATCTCCGCAC	20	59	55	382	[15]
	RV	ACGCGCTGAACAAAAGGTTC	20	59.97	50		

* RecA was used as the housekeeping gene.

Particle Size Distribution Analysis of SEAgNPs

It crucial to determine the particle size and charge of the materials before testing the antibacterial and antibiofilm properties of the synthesized SEAgNPs. According to Bhanumathi et al., the size, surface charge, shape, and composition of nanoparticles are the primary factors influencing their in vitro toxicity. 24 With the aid of the dynamic light scattering spectroscopy (DLS) method, the size and charge of the particles in an aqueous solution were identified. The surface charge and particle size distribution of the nanoparticles in solution can be easily determined using this technique. According to the DLS investigation (Figures 3A–C), the AgNPs generated from SE had an average particle size of 52.60. Particle sizes of 100 nm have great potential for biomedical applications because the type of interaction that occurs between the nanoparticles and cells is highly dependent on the size of the nanoparticles.[25]

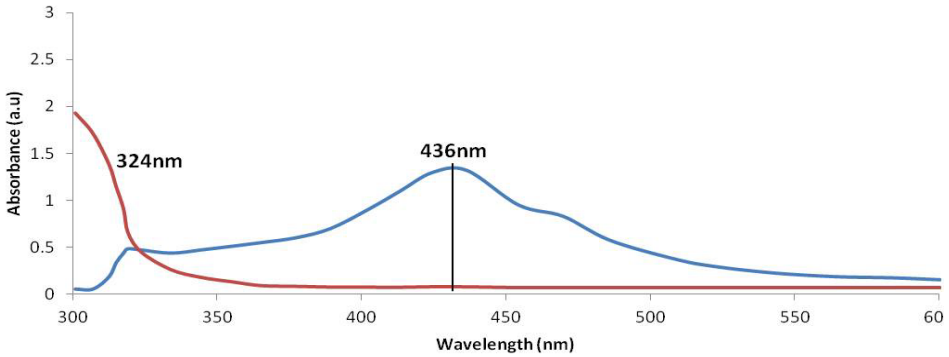

Figure 1: Blue line: UV spectra of the SEAgNPs synthesized with silkworm pellets. AgNO3 depicted in the red line. Peak of the SEAgNPs (Blue line) can be seen at 436nm.

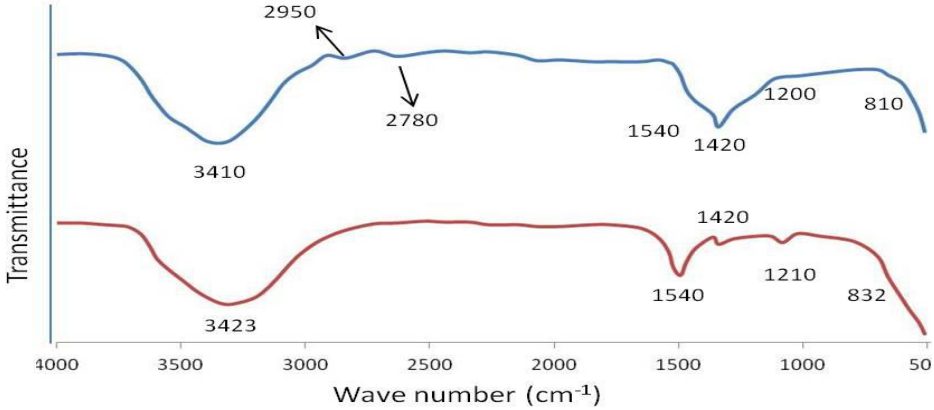

Figure 2: FTIR spectra of SEAgNPs formed from Silk worm pellets extract (SE) from 500 to 4000cm-1. Red: AgNO3; Blue: SEAgNPs

ISSN 2616-0684 (Print)
ISSN 2616-0692 (Electronic)

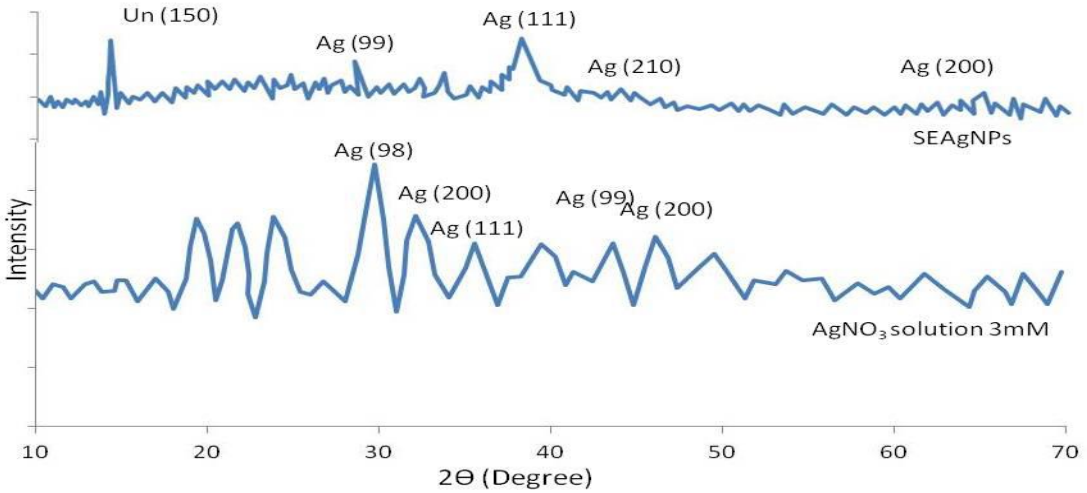

Figure 3: XRD pattern for SEAgNPs formed from Silkworm pellets extract (PE).

Antibacterial activity

SEAgNPs exhibited bactericidal activity against all the strains tested in this study. MICs of all the isolates were significant, with 54.67 ± 2.13, 78.6 ± 2.56, and 89.12 ± 3.11µg/ml respectively for SM, SO and SG. The present findings were significant to that of the positive control 18.5 ±1.11µg/ml ($P < 0.05$). MBC was found to be significantly lower in SM than in SO and SG. The MBC measured against the strains showed bactericidal effects. The MBIC50 was found to be in accordance with both MBC and MIC, wherein the concentration was significantly low (8.9 ± 1.9 for SM (MBIC50 for positive control was 4 ± 1.2).

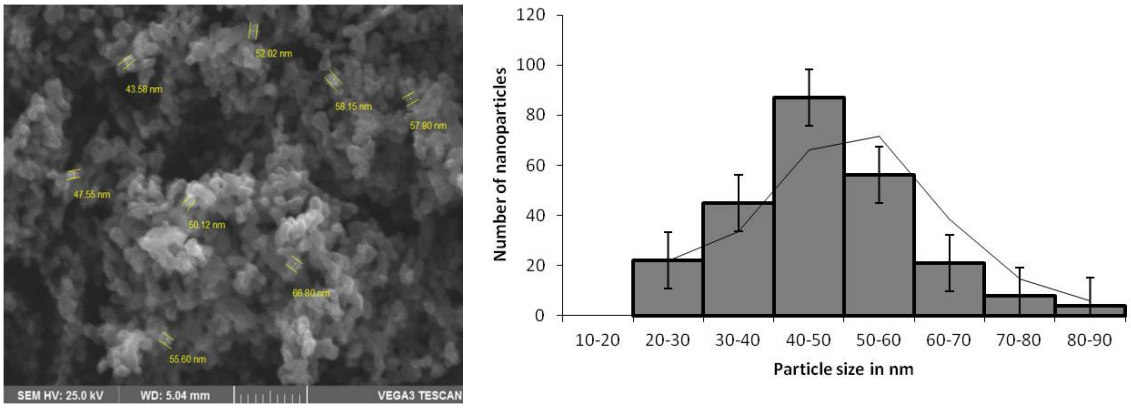

(A) (B)

Figure 4: (A) SEM images of the synthesized AgNPs and (B) a graph showing the number of nanoparticles observed at different sizes (Right). All the values are the average of triplicates and expressed as value ± SD.

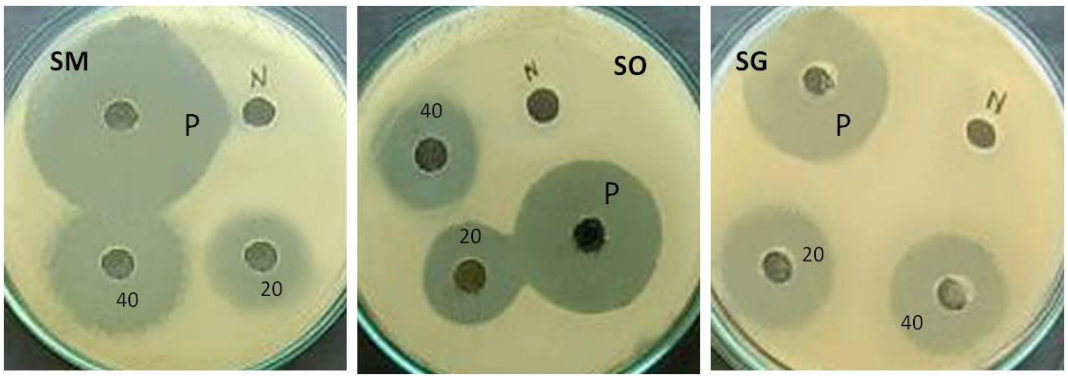

Figure 5: Agar well diffusion method showing the zone of inhibition of SM, SO, and SG strains. P: Positive control (Vancomycin); N: Negative control; 20 and 40 numbers represent 20 and 40µg/ml concentration of the test particles.

Time-kill assay

Time-killing curves of SEAgNPs against bacterial isolates at 0.5, 1, and 2 MIC were significant when compared to the control and positive controls. The activity was dose- and time-dependent ($P < 0.05$). The positive control showed complete inhibition after 30 minutes. In contrast, the 2 × MIC of SEAgNPs took 60 min to kill all SM strains. In contrast, the 2 × MIC of SEAgNPs took 90 min to kill all SO and SG strains ($P < 0.05$).

Antibiofilm by crystal violet

The synthesized SEAgNPs showed promising biofilm formation inhibition effects against all three bacterial strains compared to the positive control. The biofilm inhibition assay of SEAgNPs was the most significant against SM, followed by SO and SG. This effect was both dose- and time-dependent. These results were in accordance with those of the time-kill assay. Two-way ANOVA between the isolates and time period was conducted to compare the effect of biofilm inhibition by SEAgNPs. All the effects were statistically significant at a significance level of 0.05. There was a significant difference between incubation time and treatment ($p<0.05$ [$F(2,6) = 51.22984$, $P=0.000169$]. However, no significant differences were observed between the strains. [$F(3,6) = 3.093897$, $P= 0.111055$]. The Tukey HSD test for post-hoc comparisons revealed that the mean score differed substantially between the positive control and SEAgNP groups. The inhibition of biofilm formation in SM was found to be 56 and 94% after 12 and 24 h of incubation, respectively. The Inhibition was 100% for the positive control. Biofilm inhibition was recorded to be 78.3 and 67.8% for SO and SG, respectively, after 24 h of incubation.

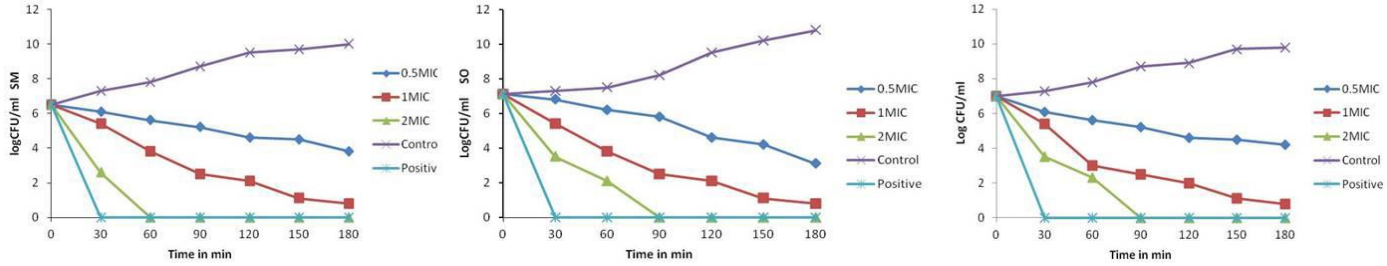

Figure 6: Scatter plots of Time kill assays of SEAgNPs against SM, SO, and SG. All the values are average of triplicates

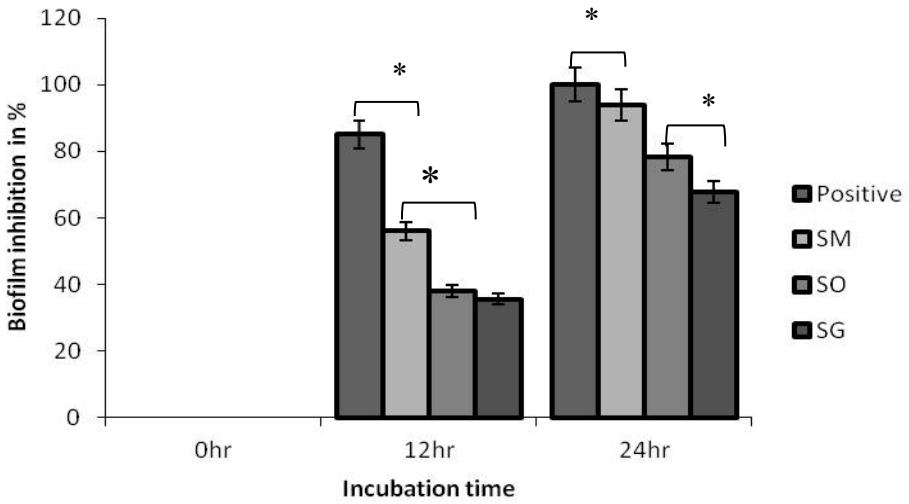

Figure 7: Biofilm evaluation by crystal violet assay. An assay was carried for 24hr incubation Vancomycin was used as a positive control. At 0 hr, the inhibition was assumed to be 0%. All the values are the average of triplicates and expressed as mean value ± SD,

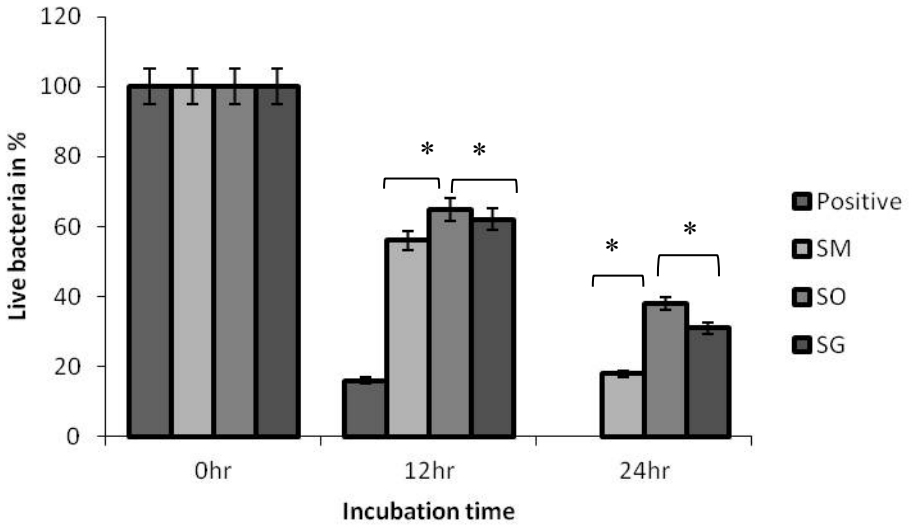

Figure 8: Biofilm evaluation by MTT assay. An assay was carried out for 24hr incubation, Vancomycin was used as positive control. At 0hr, the number of live cells were 100%. All the values are average of triplicates and expressed as mean value ± SD, * $P< 0.05$, ** $p < 0.01$, according to Tukey's post hoc test

ISSN 2616-0684 (Print)
ISSN 2616-0692 (Electronic)

Antibiofilm by MTT assay

The positive control showed a highly significant reduction in live cells to 16% at 12 h. The percentage viability of living cells was significantly reduced from 100% to 18% at 24 h in SM. This was highly significant compared with that of the positive control ($P < 0.05$). In contrast, cell viability was reduced to 38% and 31% for SO and SG, respectively. A two-way ANOVA between the isolates and the period was conducted to compare the effects of SEAgNPs on the cell viability. All the effects were statistically significant at a significance level of 0.05. There was a significant difference between incubation time and treatment ($p<0.05$ [$F(2,6) = 42.68735$, $P=0.000283$]). However, no significant differences were observed between the strains. [$F(3,6) = 3.425231$, $P= 0.09311$]. The Tukey HSD test for post-hoc comparisons revealed that the mean score differed substantially between the positive control and SEAgNP groups.

Light Microscopy of Biofilms

SEAgNPs showed an obvious inhibition of attachment at the beginning of biofilm formation. At 2MIC concentration, the attachment of the isolates to the slide was completely inhibited. This treatment resulted in reduced biofilms for all three strains; however, SM was completely disrupted, followed by SO and SG. After 24 h of incubation, complete disruption of the biofilm was observed in all the isolates ($P < 0.05$). Nevertheless disturb the 24-hour-old biofilm, leading to a decrease in biofilm thickness and disordered structures, despite the biofilm's highly organized structures.

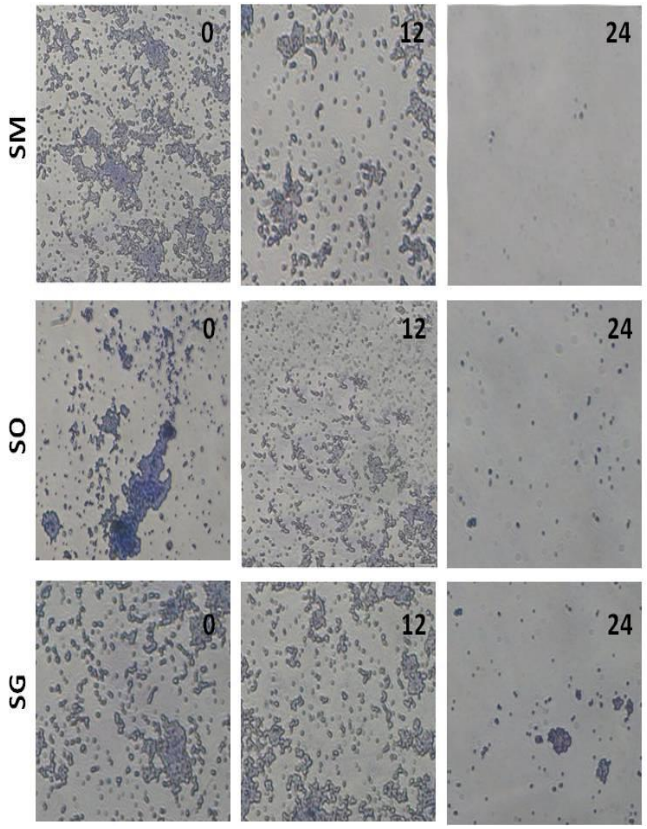

Figure 9: Light microscopy images (40x) with methylene blue staining. *S. mutans, S. oralis, S. gingivalis* can be seen after 24hr treatment with SEAgNps. All the isolates were treated at 2MIC concentration.

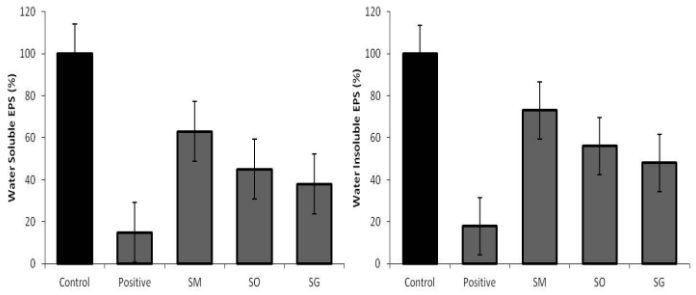

Figure 10: Percentage of EPS produced under the treatment of SEAgNPs at 0.5MIC concentration. Control (untreated strain) was assumed to be 100%. Vancomycin was used as a positive control. The untreated bacteria were served as control. $P< 0.05$ indicate the significant difference.

Extracellular Polysaccharide Production

From found that SEAgNP inhibited the production of both insoluble and soluble EPS, indicating an inhibitory or antibiofilm effect against the oral strains in this study. Inhibition was observed for all three strains ($P <0.05$). The present results were matched those of SM, SO, and SG biofilm assays. The inhibitory rates of soluble EPS were found to be 63.21 ± 1.25, 45.06 ± 1.11, and $38.65 \pm 2.8\%$ for SM, SO, and SG, respectively. The inhibition rates of water-insoluble EPS were recorded to be 73.05 ± 1.08, 56.71 ± 2.31 and $48.11 \pm 2.1\%$ for SM, SO, and SG, respectively. On the other hand, EPS inhibition was 15 and 18% for water-soluble and water-insoluble EPS inhibition, respectively ($P <0.05$).

Real-time expression

Real-time RT-PCR was used to quantify the expression of the chosen genes gftB, gftC, gftD, sortase A, comD, and the housekeeping gene recA. The pattern of gene expression, as determined by Ct values, is depicted in (Figures 11–15) and shows the downregulation of the chosen genes. The observed expression patterns matched those of in vitro biofilm inhibition studies. All the gene members were expressed at the expected base pairs, as shown in the agarose gel (Figure 16). Figures depict how SEAgNPs affected the expression of genes involved in biofilm formation and EPS production in bacterial strains. The primary building blocks of EPSs are water-insoluble polysaccharides, which are produced by the gtfB and gtfC genes, whereas water-soluble extracellular polysaccharides are produced by the gtf D gene. In the present study, the EPS-synthesizing genes Gtf B, Gtf C, and Gtf D were significantly downregulated in all bacterial strains when exposed to a 2MIC concentration of SEAgNPs ($P< 0.05$). The relative expression levels of the gtf B, C, and D genes in bacteria treated with SEAgNPs were lower than those in the control at 2MIC concentration (Figures 11-15). This difference was statistically significant in the positive control group. This downregulation was in accordance with a previous EPS inhibition assay, confirming the role of these genes in EPS production, thereby aiding biofilm formation. Similarly, gene members thought to be responsible for biofilm formation (sortase A and comD) were also found to be significantly downregulated compared to the control (1 or 100%). The downregulation was recorded to be below 0.7 (positive control below 0.4) and was seen in all three species of the study ($P <0.05$) (Figures 11-15). The present results are in accordance with those of a biofilm inhibition study.

In this study, green-synthesized AgNPs were tested as antimicrobial agents against three oral bacterial strains (*S. mutans, S. oralis* and *S. gingivalis*). The results showed that The synthesized AgNPs completely inhibited the growth of the tested bacterial strains. Inhibition of bacterial growth was dose- and time-dependent. In this study, green-synthesized AgNPs inhibited oral bacterial strains, with inhibition zones of 20, 15, and 14 mm against SM, SO, and SG, respectively ($P <0.05$). This was highly significant compared with that of the positive control (25 mm).

The MIC values were also significant, with values as low as 54.67 ±2.13 for SM when compared to the positive control (18.5 ±1.11).

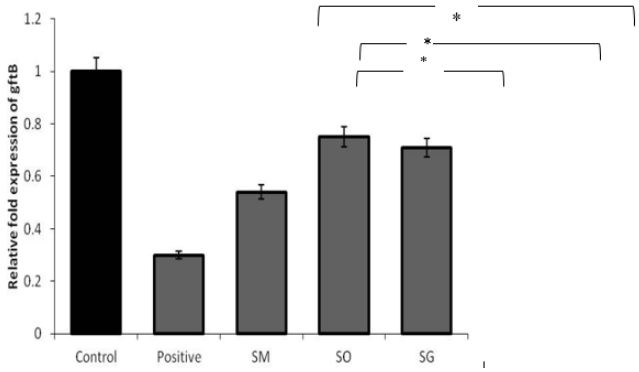

Figure 11: Graph depicting real-time RT-PCR's validation of gftB. The 2-ΔΔCt formula was used to calculate gene expression using the Ct values. RecA functions as a normalizer and a housekeeping gene. Each experiment was carried out three times.

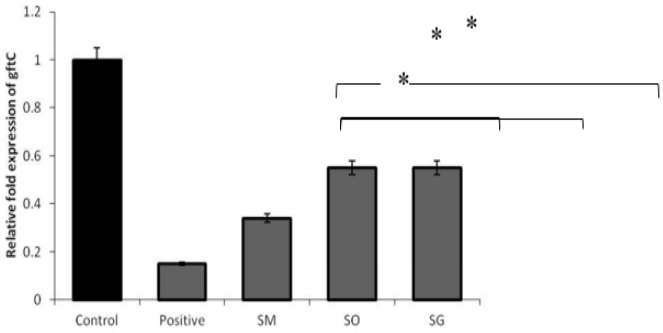

Figure 12: Graph depicting real-time RT-PCR's validation of gftC. The 2-ΔΔCt formula was used to calculate gene expression using the Ct values. RecA functions as a normalizer and a housekeeping gene. Each experiment was carried out three times.

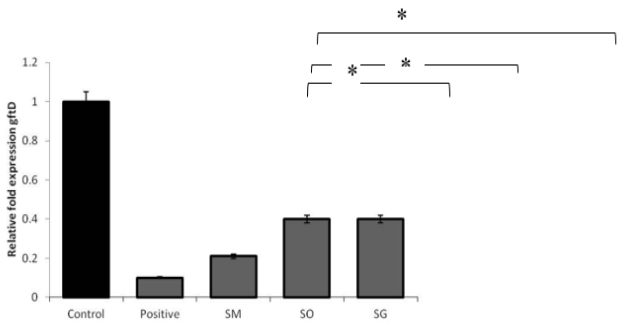

Figure 13: Graph depicting real-time RT-PCR's validation of gftD. The 2-ΔΔCt formula was used to calculate gene expression using the Ct values. RecA functions as a normalizer and a housekeeping gene. Each experiment was carried out three times.

Throughout this study, the antibacterial activity was significantly higher against SM than against the other two strains (SO and SG). The evaluation of the antibacterial activity of AgNPs, along with many green-synthesized AgNPs, has been studied by many biologists, but the green synthesis from silkworm pellets was reported for the first time. AgNPs successfully inhibited and killed bacteria in a dose- and time-dependent manner, as revealed in time-kill assays; however, the bacterial reproduction time may be an appropriate strategy to prevent viable infection. To cling to the tooth surface and create cariogenic biofilms, *S. mutans* or other oral bacteria require the presence of bacterial EPSs. Glucosyltransferases (GTFs) produce EPSs, which are important for biofilm generation and maintenance.

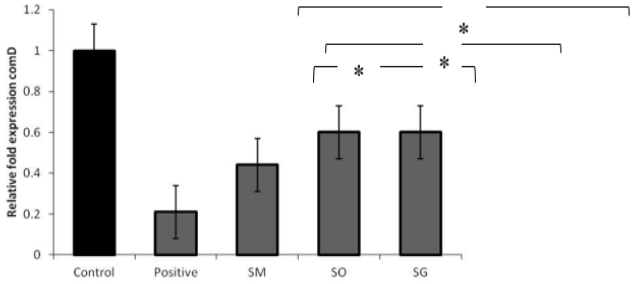

Figure 14: Graph depicting real-time RT-PCR's validation of comD. The 2-ΔΔCt formula was used to calculate gene expression using the Ct values. RecA functions as a normalizer and a housekeeping gene. Each experiment was carried out three times.

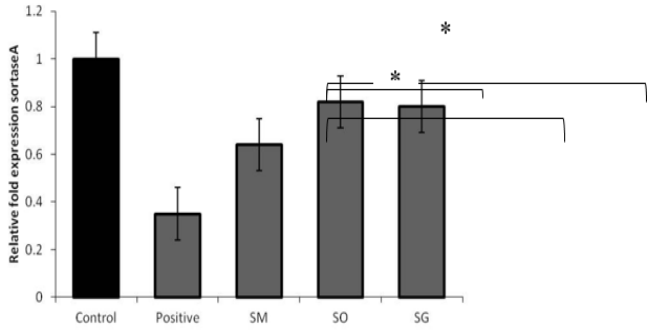

Figure 15: Graph depicting real-time RT-PCR's validation of sortase A. The 2-ΔΔCt formula was used to calculate gene expression using the Ct values. RecA functions as a normalizer and a housekeeping gene. Each experiment was carried out three times.

In a dose-dependent manner, AgNPs may block the synthesis of both water-soluble and water-insoluble EPS, which was evident in present EPS study. EPS was inhibited at rate of 63.21 ±1.25, 45.06 ±1.11, and 38.65 ± 2.8% for SM, SO, and SG, respectively, in the case of soluble EPS. In contrast, the inhibition rates of water-insoluble EPS were found to be 73.05 ±1.08, 56.71 ±2.31, and 48.11 ± 2.1% for SM, SO, and SG, respectively. Similar results were obtained in studies conducted on biofilm matrices of oral bacteria.[20] Antibiofilm studies were done by

crystal violet, MTT, and light microscopy. After 24 h of incubation, the viability percentage of living cells was significantly reduced to 18% in the presence of 100% SM. This was highly significant when compared with that of the positive control, which was 16% ($P < 0.05$). Percentage viability was estimated using the MTT assay.

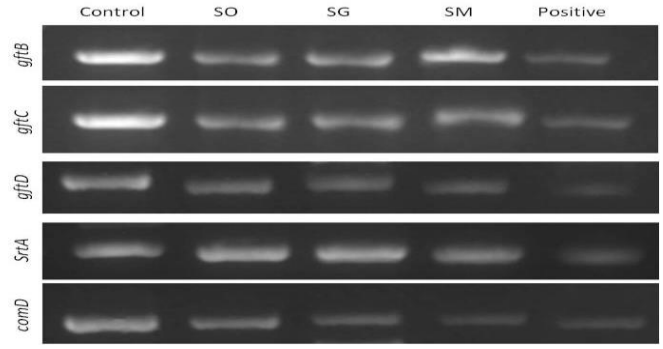

Figure 16: Photographic images of the expressed gene members by Real time PCR on 1% agarose gel. Control: without treatment; Vancomycin is used as positive control. gftB, gftC, gftD, srtA and comD were found to be 240, 210, 150, 470, and 217bp, respectively. All the gene members were expressed at expected length.

Similar results were observed in the crystal violet assay, where the inhibition was 56 and 94% after 12 and 24 h incubation, respectively. After 24 h of incubation, the biofilm was completely disrupted, as observed using light microscopy. Similar antibiofilm reports were observed where *S. mutans* biofilms were inhibited by antimicrobial peptides; [26] biofilms in the case of dental caries caused by *Streptococcus mutans* were found to be greatly inhibited by several external agents, such as metallic nanoparticles, plant extracts, [27] and other purified antimicrobial peptides.[28] The current real-time RT-PCR data to quantify the expression of biofilm formation genes (gftB, gftC, gftD, sortase A, and comD) showed a significant downregulation of these genes. This downregulation may be the sole reason for the observed reductions in biofilm formation and EPS secretion. Similar data were reported by Koo et al.,[29] who observed a significant downregulation of the exopolysaccharide matrix. *Streptococcus mutans* gtf C gene member responsible for the synthesis of both soluble and insoluble glucans was reported to be downregulated, similar to the current findings.[30]

Table 2: Table showing the inhibition zone, MIC, MBC, and MBIC50 values of the SEAgNPs against the oral bacterial strains in the study ($P<0.05$), values sharing different superscript letters (a, b, c) are significantly different at $P< 0.05$ by Tukey's post hoc test

	Zone of inhibition in mm	MIC μg/ml	MBC μg/ml	$MBIC_{50}$ μg/ml
Positive	25 ±1.06^a	18.5 ±1.11^a	10 ± 2.11^a	4 ± 1.2^a
SM	20 ±1.2^b	54.67 ±2.13^b	35 ± 3.41^b	8.9 ± 1.9^b
SO	15 ±1.5^c	78.6 ±2.56^c	63 ± 3.11^c	12.1 ± 2.3^c
SG	14 ±1.1^c	89.12 ± 3.11^c	75 ± 2.78^c	13.4 ± 2.4^c

Values are presented as the mean ± SD. Different superscript letters (a, b, c) in the same column indicate statistically significant differences between treatments ($P< 0.05$), as determined by Tukey's post hoc test.

Conclusion

The green-synthesized AgNPs from Silkworm excreta exerted antimicrobial activity against all the oral bacterial strains, *S. mutans*, *S. oralis* and *S. gingivalis*. Antibacterial activity was confirmed by MIC, biofilm inhibition, and time-kill assays. The extracellular polysaccharide content decreased proportionately with the dosage of AgNPs and the incubation time. Several studies have confirmed its possible role in biofilm stabilization. AgNPs also impeded biofilm attachment by the strains in attachment *in-vitro* which might be due to the downregulation of *gtfs, sortase A* and *comD* genes. As stated earlier, these genes aid biofilm formation and stabilization. These findings show that AgNPs drastically reduce or completely eradicate medication resistance, and provide a new approach for managing plant pathogens. AgNPs soon undergo changes in their surface charge, acid-base properties, and aggregation behavior, and their effects on the antibacterial activity of AgNPs will be evaluated.

Conflicts of Interest

The authors declare no conflicts of interest.

Authors' Declaration

The authors hereby declare that the work presented in this article is original and that any liability for claims relating to the content of this article will be borne by them.

Acknowledgments

Gratitude and appreciation are extended to Al-Mustansiriya University/ College of Pharmacy for the facilitation of this work in their laboratories.

References

1. Selwitz RH, Ismail AI, Pitts NB. Dental caries. The Lancet. 2007;369(9555):51-59.
2. Yu OY, Lam WY-H, Wong AW-Y, Duangthip D, Chu C-H. Nonrestorative management of dental caries. Dent. J. 2021;9(10):121.
3. Featherstone J. The continuum of dental caries—evidence for a dynamic disease process. J. Dent. Res. 2004;83(1_suppl):39-42.
4. Thomas B, Ramesh A. Nanotechnol. Dent. Implantol. Nanomaterials in Dental Medicine: Springer; 2023. p. 159-175.
5. Hannig M, Hannig C. Nanotechnology and its role in caries therapy. Adv. Dent. Res. 2012;24(2):53-7.
6. Hoque J, Konai MM, Sequeira SS, Samaddar S, Haldar J. Antibacterial and antibiofilm activity of cationic small molecules with spatial positioning of hydrophobicity: an in vitro and in vivo evaluation. J. Med. Chem. 2016;59(23):10750-62.
7. Zhang B, Zhao M, Tian J, Lei L, Huang R. Novel antimicrobial agents targeting the Streptococcus mutans biofilms discovery

through computer technology. Front. Cell. Infect. Microbiol. 2022;12:1808.
8. Kouidhi B, Al Qurashi YMA, Chaieb K. Drug resistance of bacterial dental biofilm and the potential use of natural compounds as alternative for prevention and treatment. Microb. Pathog. 2015;80:39-49.
9. Karibasappa G, Sujatha A. Antibiotic resistance-a concern for dentists. J. Dent. Med. Sci. 2014;13(2):112-118.
10. Kaur N, Sahni P, Singhvi A, Hans MK, Ahluwalia AS. Screening the drug resistance property among aerobic pathogenic microorganisms of dental caries in north-western Indian population: a preliminary study. J. Clin. Diagn. Res. 2015;9(7):ZC05.
11. Solomon SL, Oliver KB. Antibiotic resistance threats in the United States: stepping back from the brink. Am. Fam. Physician. 2014;89(12):938-41.
12. Chater AM, Family H, Abraao LM, Burnett E, Castro-Sanchez E, Du Toit B, et al. Influences on nurses' engagement in antimicrobial stewardship behaviours: a multi-country survey using the Theoretical Domains Framework. J. Hosp. Infect. 2022;129:171-80.
13. Piddock LJ. The crisis of no new antibiotics—what is the way forward? Lancet Infect. Dis. 2012;12(3):249-253.
14. Bakhshi B, Malla S, Gowda LS. Garlic Mediated Green Synthesis of Silver Nanoparticles as Antifungal Agents against Magnaporthe oryzae. Indian J. Pharm. Educ. Res. 2022;56(4).
15. Sudhakar M, Raman BV. Bactericidal and Antibiofilm Activity of Tannin Fractions Derived from Azadirachta against Streptococcus mutans. Asian J. Appl. Sci. 13: 132-143 DOI: 103923/ajaps. 2020;143.
16. Sutthisa W, Sophachan H, Pimvichai P, Srisawad N. Antimicrobial Efficiency and Chemical Composition of Jackfruit (Artocarpus heterophyllus Lam.) Extracts from Different Plant Parts. Trop. J. Nat. Prod. Res. 2025;9(3):925-32.
17. Thammawithan S, Siritongsuk P, Nasompag S, Daduang S, Klaynongsruang S, Prapasarakul N, Patramanon R. A biological study of anisotropic silver nanoparticles and their antimicrobial application for topical use. Vet. Sci. 2021;8(9):177.
18. Mishra B, Wang X, Lushnikova T, Zhang Y, Golla RM, Narayana JL, et al. Antibacterial, antifungal, anticancer activities and structural bioinformatics analysis of six naturally occurring temporins. Peptides. 2018;106:9-20.
19. Packiavathy IASV, Priya S, Pandian SK, Ravi AV. Inhibition of biofilm development of uropathogens by curcumin–an anti-quorum sensing agent from *Curcuma longa*. Food Chem. 2014;148:453-460.
20. Gulube Z, Patel M. Effect of *Punica granatum* on the virulence factors of cariogenic bacteria *Streptococcus mutans*. Microb. Pathog. 2016;98:45-9.
21. Livak KJ, Schmittgen TD. Analysis of Relative Gene Expression Data Using Real-Time Quantitative PCR and the 2−ΔΔCT Method. Methods. 2001;25(4):402-408.
22. Augustine R, Rajarathinam K. Synthesis and characterization of silver nanoparticles and its immobilization on alginate coated sutures for the prevention of surgical wound infections and the in vitro release studies. 2012.
23. Thamilselvi V, Radha K. Synthesis of silver nanoparticles from *Pseudomonas putida* NCIM 2650 in silver nitrate supplemented growth medium and optimization using response surface methodology. Dig. J. Nanomater. Biostruct. 2013;8(3).
24. Bhanumathi R, Vimala K, Shanthi K, Thangaraj R, Kannan S. Bioformulation of silver nanoparticles as berberine carrier cum anticancer agent against breast cancer. New J Chem. 2017;41(23):14466-77.
25. Jeevanandam J, Barhoum A, Chan YS, Dufresne A, Danquah MK. Review on nanoparticles and nanostructured materials: history, sources, toxicity and regulations. Beilstein J. Nanotechnol. 2018;9(1):1050-1074.
26. Wang Y, Zeng Y, Wang Y, Li H, Yu S, Jiang W, et al. Antimicrobial peptide GH12 targets Streptococcus mutans to arrest caries development in rats. J. Oral Microbiol. 2019;11(1):1549921.
27. Gazoni VF, Balogun SO, Arunachalam K, Oliveira DM, Cechinel Filho V, Lima SR, et al. Assessment of toxicity and differential antimicrobial activity of methanol extract of rhizome of Simaba ferruginea A. St.-Hil. and its isolate canthin-6-one. J. Ethnopharmacol. 2018;223:122-134.
28. Li L, Sun J, Xia S, Tian X, Cheserek MJ, Le G. Mechanism of antifungal activity of antimicrobial peptide APP, a cell-penetrating peptide derivative, against Candida albicans: intracellular DNA binding and cell cycle arrest. Appl. Microbiol. Biotechnol. 2016;100:3245-53.
29. Koo H, Falsetta M, Klein M. The exopolysaccharide matrix: a virulence determinant of cariogenic biofilm. J. Dent. Res. 2013;92(12):1065-73.
30. Hanada N, Kuramitsu HK. Isolation and characterization of the *Streptococcus mutans* gtfC gene, coding for synthesis of both soluble and insoluble glucans. Infect. Immun. 1988;56(8):1999-2005.
31. Zhong H, Xie Z, Wei H, Zhang S, Song Y, Wang M, Zhang Y. Antibacterial and antibiofilm activity of Temporin-GHc and Temporin-GHd against cariogenic bacteria, *Streptococcus mutans.* Front. Microbiol. 2019;10:2854.